THE ADSORPTION OF AMOXICILLIN BY MESOPOROUS SILICA SUPPORTED POLYMERS

By

YUE SONG

A thesis submitted to the

School of Graduate Studies

Rutgers, The State University of New Jersey

In partial fulfillment of the requirements

For the degree of

Master of Science

Graduate Program in Chemical and Biochemical Engineering

Written under the direction of

Tewodros Asefa

and approved by

_____

_____

_____

New Brunswick, New Jersey

January 2018

ABSTRACT OF THE THESIS

The Adsorption of Amoxicillin by Mesoporous Silica Supported Polymers

By: YUE SONG

Thesis Director:

Prof. Tewodros Asefa

The emerging pollutants (EPs) originated from our fast developing modern society possess potential threat to human health and environment. Among many sources of EPs, regular as well as abusive use of antibiotics such as amoxicillin (AMX) has gained more attentions in recent years. However, corresponding treatment plan toward EPs is still in its infancy. On the other hand, novel nanomaterial (mesoporous silica supported polymers), which possess large surface area and amendable surface characteristics, can be used as adsorbent to remove EPs such as AMX. In this study, mesoporous silica supported polymers (H^+-PANI/SBA-15 and PANI/SBA-15) were synthesized and demonstrated to adsorb AMX from solutions with different initial pH values and initial concentrations. Data were collected through UV-Vis spectrometer and pH meter. The material suitable for adsorbing AMX was found to be H^+-PANI/SBA-15 under initial pH around 11.0 and with final pH around 7.0. The experimental adsorption data were modelled using pseudo-second order and intraparticle diffusion models and adsorption mechanisms were discussed as well.

Acknowledgement

First of all, I would like to thank my adviser Prof. Tewodros Asefa for his guidance, patience and great inspiration he provided during my research. He consistently allowed this paper to be my own work, but assisted me in the right direction whenever he thought I needed it. I would also like to thank Prof. Rohit Ramachandran and Prof. Haoran Zhang for being members of my thesis committee.

I also appreciate the help and kindness from my colleagues in this research group. I would like to thank Tao Zhang, Dr. Xiaoxi Huang, and Prof. Vitor C. Almeida for their help with the scientific discussion and instrument operation.

Finally, I must express my very profound gratitude to my parents and to my fiancé, Lu Wang, for providing me with unfailing support and continuous encouragement throughout my years of study. This accomplishment would not have been possible without them. Thank you.

Table of Contents

Abbreviations

μm……...Micrometer

nm ...……Nanometer

EPs…….……Emerging pollutants

AMX …….…….....Amoxicillin

year^{-1} ……Per year

PANI ……..……..Polyaniline

H^+-PANI ……...Protonated polyaniline

SBA-15 ……..Santa Barbara amorphous type material

H^+-PANI/SBA-15 ….……..SBA-15 supported polyaniline nanocomposite

Pluronic® P-123….....Poly(ethylene glycol)-block-poly (propylene glycol)-block-poly(ethylene glycol)

TEOS……Tetraethyl orthosilicate

mL ……Milli liter

h……Hour

g…….....Gram

°C ……..Degree Celsius

mmol…….....Milli mole

M……Molar per liter

mg……Milli gram

Fig ……...Figure

pka……Acid dissociation constant

min ……Minute

nm ……Nanometer

C_t ……...AMX concentration in solution at time t

t…….....time

λ_c……Absorbance of nanocomposite

λ_t ……..Absorbance at time t

m_t ……...Mass of AMX being adsorbed at time t

C_0…….AMX initial concentration

V ……..…….Volume

L…….Liter

pH_i……..Initial pH

pH_f ……..Final pH

m_e ……...…….……Mass of adsorbed AMX at equilibrium

m_i…….……..Mass of initial AMX concentration

%……...Percent

µg……...Micro gram

W…….……Mass of adsorbent

q_t …….……Amount of AMX adsorbed per milligram of adsorbent

R^2……..Correlation coefficient

vs ……..……...……Versus

k_2 …….……...Rate constant of pseudo-second order model

k_i …….……..Rate constant of intraparticle diffusion model

List of Tables

List of Illustrations

Chapter 1

1.1. Nanomaterials

Nanomaterials describe materials that have structural components smaller than 100 nm in at least one dimension. Many researchers limit the size of nanomaterials to 50 nm or 100 nm[1] based on the fact that some physical properties of some nanoparticles approach those of the bulk at this upper limit. However, this size threshold varies with different materials and should only apply to certain types of material under certain circumstances.

The description of nanoparticles is similar to nanomaterials, which describe nanoparticles are particles with at least one dimension smaller than 100 nm, and potentially as small as atomic and molecular length scales (~0.2 nm). Nanoparticles have different morphological characteristics to be taken into account, such as flatness, aspect ratio and sphericity. High- and low-aspect ratios are generally used to classify nanoparticles. High aspect ratio nanoparticles include nanorods and nanowires while oval and cubic shape belong to low-aspect-ratio particles. In some reports[1, 3], nano-particulate matters are considered as a distinct state of matter besides solid, liquid, gas and plasma, due to its characteristic properties (large surface area and quantum size effect).

Compared with microparticles or bulk materials, nanoparticles have higher fraction of atoms at its surface and thus possess much larger surface area. These factors could significantly enhance nanoparticle's chemical reactivity, roughly 1000-fold or more, for example. With high surface areas and special surface chemical properties, they can be used as carriers or binding site for gas, liquid and other forms of chemical compounds. As a result, nanomaterials provide a platform for cultivating and practicing new ideas and

novel technologies in different fields.

Nanotechnology (nanotech) is manipulation of matter on an atomic, molecular, and supramolecular scale. The earliest, widespread description of nanotechnology[2, 3] referred to the particular technological goal of precisely manipulating atoms and molecules for fabrication of macroscale products, also now referred to as molecular nanotechnology. This idea was first put forward by Feynman at the December 1959 meeting of the American Physical Society[1], where he asked "What would happen if we could arrange the atoms one by one the way we want them?". However, nanomaterials did not first come into existence with the emergence of nanotechnology. Nanomaterials are abundant in nature since they can be easily produced in many natural processes.

Recent advances in nanomaterial synthesis and characterization devices have given strong support to the industrial use and academic study of nanostructured materials. Applications of nanoparticles are now booming in many different industries, including but not limited to electronics, transportation and telecommunication, biomedical applications and pollution remediation. For example, in biomedical applications, researchers have been trying to harness the ability of nanoparticles to target and penetrate specific organs and cells for drug delivery purpose and achieve sustainable controlled drug release. In the research of environment remediation and pollutants removal, nanomaterials with high surface area have been exploited to catalyze and degrade pollutants under certain conditions or to serve as absorbents to physically remove pollutants from the environment.

1.2. Emerging Pollutants

As human society keep developing in fast pace, the quantity and diversity of pollutants are growing correspondently. Emerging pollutants (EPs), also called emergent contaminants, have drawn a lot of attention in recent years. By definition, EPs can be broadly defined as synthetic or naturally occurring chemicals that are not commonly monitored in the environment but which have the potential to enter the environment and cause known or suspected adverse ecological and human health effects[4]. Generally, EPs correspond to unregulated pollutants, which may possibly be regulated in the future based on the studies of their environmental impact and health effect.

At present, there are more than 700 substances that are categorized as EPs (e.g. pharmaceuticals, pesticides, industrial wastes and municipal refuses). Most of them haven't been listed in many nations' routine monitoring programs due to their unclear transformation path, degradation and eco-toxicological effect in nature. One primary concern associated with EPs is the inadequate knowledge of EPs' long-term impact on human health, environment and aquatic life. In many cases, low concentration of EPs in the environment can be very challenging for existing detection method to identify. Meanwhile, they do not need to maintain their forms in the surrounding environment for long, because their high transformation/removal rates can be timely replenished with continuous feed from various sources.

EPs can be discharged from point (mostly urban or industries) or diffuse (agricultural waste) pollution and then being transported through different ways such as runoff, leaching and erosion into soil, rivers, ponds and other natural environments. The release patterns of EPs strongly depend on their individual properties (like polarity, functional

groups, persistence) which generate more difficulties in EPs detection method and risk assessment.

In urban areas, effluent containing EPs from waste-water treatment plants and industrial waste are being let out into natural water bodies and lands. Once reaching out to the environment, some EPs will go through degradation and transformation quickly under effects of microorganism, light, oxidation and so on; while some other EPs will persist. It would be ideal if every EPs can be biodegraded and transformed into environmental friendly substances. However, biodegradation relies on the synergy of a community of microorganism which are able to uptake EPs through their metabolic networks and this process varies significantly between compounds and has not been carefully studied.

In rural areas, modern intensive agricultural activities (livestock, crop farming) adopt antibiotics and pesticide to prevent and eliminate infectious diseases between livestock and the spreading of pests. However, in many cases, antibiotics can only be utilized in vivo to some extent and the residues will be excreted through urine and faeces while maintaining its original or in ionized and conjugated forms. A large portion of these metabolites containing antibiotics and pesticide will be spread over the land for fertilization. Once being released to the land, those EPs will find their way (e.g. runoff, leaching) into the nature. The adsorption and desorption behavior of EPs is not only depended on the pollutants intrinsic physical-chemical properties, but also vary greatly with the interacting substances (e.g. soil type, particle sizes, density). As a result of these wide range variables, EPs' environmental behavior has not been broadly studied and much of the knowledge is still unknown.

Despite the difficulty in finding EPs transport behavior in the nature, another hurdle lies in detection method limitations. There exist a number of EPs that could affect the soil and aquatic environment at extremely low concentration but the current detection limits for them are too high to allow appropriate risk assessment. In addition, EPs may have periodic or irregular shifts over time due to seasonal changes, product replacement, market demand and so on. What's more, different types of EPs have different physical and chemical characteristics such as particle size, polarity, toxicity and persistence in natural environment. All these factors together further complicate the detection method and make it harder for daily routine sampling and assessment.

Although much attention has been paid to the problems associated with EPs, with some involving scientific studies, measurement for controlling EPs generation and spreading to nature environment is still in its infancy. Urban and hospital effluent containing surfactants, pharmaceuticals, personal care products and many other groups of compounds usually ended up in wastewater treatment plant where the treatment for EPs is based on dilution of mixing different source of effluent. This method does not provide an effective way to separate EPs from its original sources because conventional treatments are not specifically designed to efficiently remove EPs.

1.3. Applications of Nanomaterials in Emerging Pollutants Control

The appealing characteristics such as high surface area-to-mass ratio, high reactivity and easy modification possessed by nanomaterials draw much attention to apply them in various fields and particularly in environmental remediation and pollutant control. The structures, shapes and physicochemical properties of nanomaterials direct their usage and capabilities. Some nanomaterials exhibit greater sensitivity in detection and removal of pathogens in pharmaceutical industries and hospital waste water treatment process. Metal and metal oxide nanomaterials are being used to catalyze and remove some organic pollutants; Nanomembranes have been applied to produce potable water, the removal of heavy metals and dyes and nanoporous materials are being studied for in vivo drug delivery systems.

Despite the inherent advantages of nanomaterials, nanoparticles also have high mobility in solution due to their nanoscaled sizes. This characteristic is favorable for applications in water purification and contaminants adsorption because the whole solution volume can be scanned and cleaned quickly. After the target substances being adsorbed, applying affordable centrifugal or magnetic force can separate the nanoparticles from the solution and concentrate contaminants in other places. It is even possible to make those nanoparticles desorb contaminants under certain conditions and recycle them to use again.

Chapter 2

2.1. Introduction

Antibiotics are kind of drugs used most widely and very frequently to treat bacterial infections of both human and agricultural livestock. The presence of antibiotics has significantly increased human life span and improved life quality. However, as we enjoy the convenience and well-being brought by antibiotics and other drugs, the large quantity of antibiotics consumed each year deserve more of our attentions to their environmental problems. Among those large-scale production of antibiotics, amoxicillin (AMX) is one of the top ten most frequently consumed drug that also has significant ecotoxicity[5], such as being toxic to several types of alga[6]. The pathway to introduce AMX to the environment is through human and livestock metabolite activities. AMX and its kind, as much as 90% of orally administered dose may remain un-degraded, being excreted through urine and feces as active compounds[7]. There is an estimation that up to 86 ± 8% of 500 mg of AMX by oral administration in humans will result in the excretion through urine after two hours of consumption[8]. Those excreted active AMX along with other antibiotics will finally enter the environment through either urban effluent or agricultural waste-storage structures.

AMX is linked to the formation of antibiotic-resistant species in waste water treatment plants. The development of those species is promoted by trace antibiotic concentrations in anaerobic and fixed film configurations which typically have high cell residence times[9]. Several techniques have been studied to remove AMX from environment and adsorption has been proven an effective method to eliminate different antibiotics from contaminated environments.

Polyaniline (PANI) is one of the most important polymers with high electrical conductivity. It was discovered 150 years ago[10], but only after the early 1980s PANI has received intense interest as conductive polymers with appealing characteristics such as facile synthesis, low-cost, environmental stability and unique optical, electrical properties. Besides PANI's major development in electrical and sensor applications, there is an increasing interest on its absorbing ability due to its easy transition between protonated (emeraldine salt or H^+-PANI) and deprotonated (emeraldine base or PANI) forms. It has been reported that H^+-PANI can be used to selectively adsorb anionic dye from solutions[11]. Although PANI films can be produced on virtually any material that is stable in the reaction medium[12], the closely compacted polymeric chains in them limit their available adsorption capacity.

SBA-15 (Santa Barbara Amorphous type material) is one of the most widely studied mesoporous silica materials with hexagonally ordered tubular channels with pores varying from 5 to 30 nm. This unique structure endows SBA-15 with large surface area-to-mass ratio and good stability. What's more, SBA-15 can be functionalized with metal ions and organic groups for various applications such as catalysis, electrochemical sensors and absorbent. It has been reported that SBA-15 supported PANI nanocomposite (H^+-PANI/SBA-15) can be used to efficiently extract anionic dyes from solutions[13] or as a novel solid-phase microextraction fiber coating[14]. However, the adsorption properties of mesoporous silica-supported PANI for antibiotics in solution has been rarely reported.

This experiment investigates in the adsorptive interaction between antibiotic AMX and polymer nanocomposite-supported mesoporous silica materials that are acid modified and not modified (H^+-PANI/SBA-15 and PANI/SBA-15) in different solutions with

different pH levels. The adsorption kinetics of AMX in H^+-PANI/SBA-15 is also studied. The synthesis of SBA-15-supported polyaniline composites is included as well.

2.2. Experimental Section

2.2.1. Materials and reagents

Poly(ethylene glycol)-*block*-poly (propylene glycol)-*block*-poly(ethylene glycol) ($(PEG)_{20}(PPG)_{70}(PEG)_{20}$ or Pluronic® P-123) with an average molecular weight of 5800 was obtained from BASF. Aniline, hydrochloric acid (ACS Reagent, 37%), tetraethyl orthosilicate (98%, TEOS), ammonium persulfate, sodium hydroxide, and amoxicillin were purchased form Sigma-Aldrich. Anhydrous ethanol was purchased from Fischer Scientific. Deionized water was used in all the experiments.

2.2.2. Synthesis of SBA-15 mesoporous silica

The synthesis of SBA-15 first involved using 4 g Pluronic® 123 as template, which was dissolved in a solution containing 20 mL concentrated hydrochloric acid and 130 mL deionized water in a plastic container. This mixture was kept stirring at 45 °C for 2 h or until Pluronic® 123 had completed dissolved. Then 8.5 g TEOS was added drop-wise into the solution and kept stirring vigorously at 45 °C for 20 h to form a gel. Subsequently, the solution in the plastic container was put into oven at 80 °C for 24 h under static condition to allow crystallization. The solution was filtered and repeatedly washed with deionized water and followed by drying at 60 °C in the oven to get white precipitate, the as-synthesized SBA-15. The as-synthesized SBA-15 was further calcined at 550 °C for 5 h to remove the template (Pluronic® 123) in order to obtain desired mesoporous SBA-15 silica material.

2.2.3. Synthesis of H^+-PANI/SBA-15 and PANI/SBA-15

First, 150 mg SBA-15 was added into 30 mL deionized water and dispersed uniformly through sonication. Next, 0.3 mL (3.28 mmol) of aniline was slowly added to the above suspension to form a mixture and was stirred for 4 h at room temperature. Hydrochloric acid (1 M) was used to adjust the suspension's pH to 4.0 and followed by another 4 h stirring in ice bath (0-5 °C) to disperse protonated aniline uniformly through the pores and surface of SBA-15. After 4 h of stirring, ice bath continued and the oxidant solution of 750 mg ammonium persulfate (3.28 mmol) dissolved in 1 mL deionized water was slowly drop-wise added into the suspension. Immediately, the polymerization of aniline started to take place as indicate by the color change from white to dark green. The reaction was continued for 10 h for better polymerization of aniline and better coating on SBA-15's surface. In the end, the solid product (H^+-PANI/SBA-15) was collected by centrifugation and washed with deionized water and ethanol many times until the supernatant became clear. The resulting solid, dark green product was the emeraldine salt of PANI coated onto SBA-15, named H^+-PANI/SBA-15.

The preparation of PANI/SBA-15 (the emeraldine base form of PANI supported onto SBA-15) was based on the transformation of H^+-PANI/SBA-15. First, 20 mg of H^+-PANI/SBA-15 was added into 40 mL sodium hydroxide solution (0.1 M) and kept stirring for 1 h. A color change can be observed from dark green to dark blue, indicating the transformation of H^+-PANI/SBA-15 toward PANI/SBA-15. The suspension was centrifuged to get recovered precipitate and then washed with deionized water and ethanol. The obtained PANI/SBA-15 was let to dry and stored for further use.

2.3. Results and Discussions

2.3.1. Test of AMX UV-Vis absorbance under different pH

AMX ($C_{16}H_{19}N_3O_5S$, Fig. 1) is a water-soluble compound (3430 mg/L at 20 °C) and susceptible to protonation and deprotonation in solution due to its multiple functional groups such as carboxyl (pka_1 = 2.68), amine (pka_2 = 7.49) and phenolic (pka_3 = 9.63). As a result, AMX has different chemical structures under different pH values, which may potentially affect its UV-Vis absorbance. Therefore, to validate AMX, measuring the UV-Vis absorbance under different pH values is necessary.

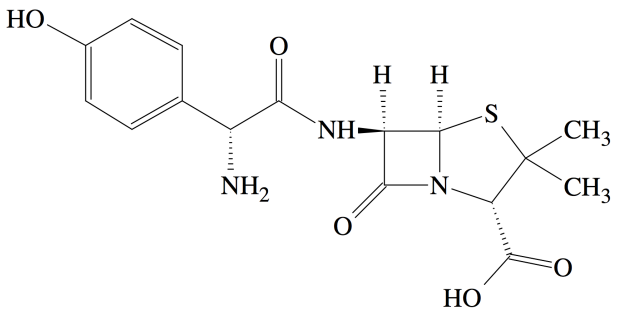

Fig. 1. Molecular structure of AMX. [15]

Deionized water was used as solvent to dissolve AMX in order to prepare stock solution and samples. In this test, 20 mL of AMX solution at the concentration of 40 mg/L (diluted from stock solution) were used in this test. Hydrochloride acid (0.1 M) and sodium hydroxide solution (0.1 M) were used for balancing solution's pH. The pH values from different solutions throughout the entire experiment were measured using Accumet pH meter 915 (Fisher Scientific). Samples were taken for UV-Vis analysis and then put back at 10 min, 30 min, 240 min, 360 min and 1200 min.

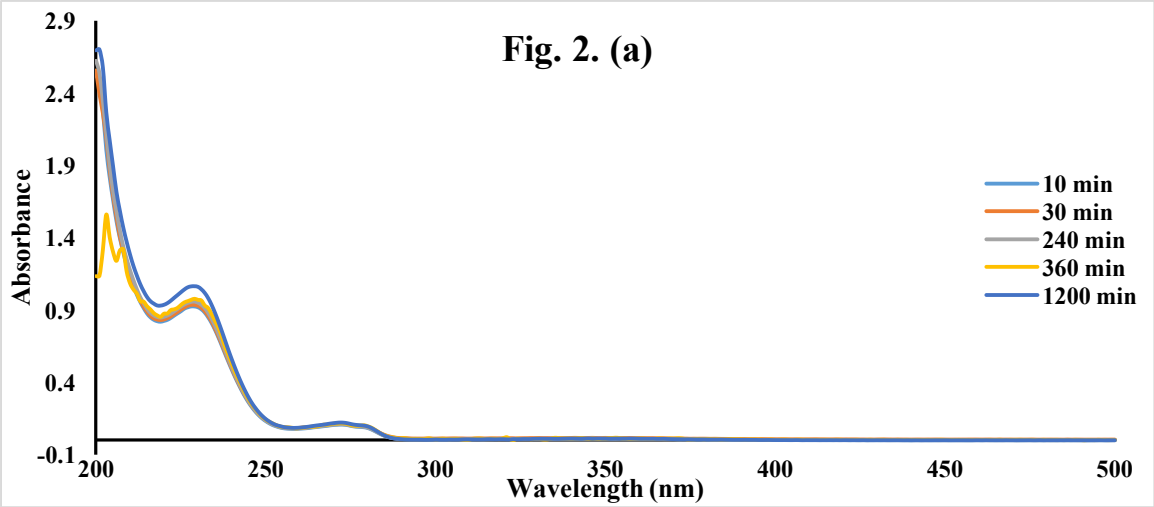

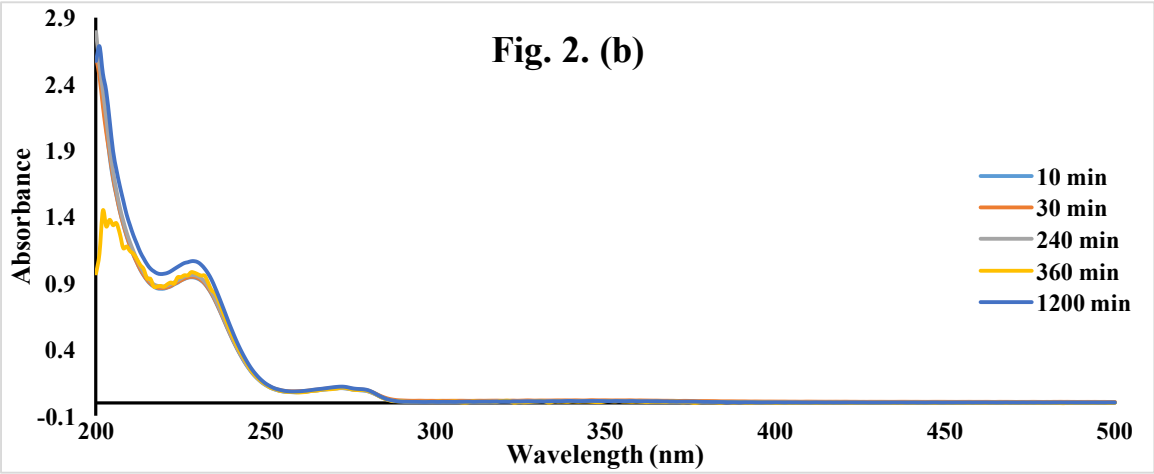

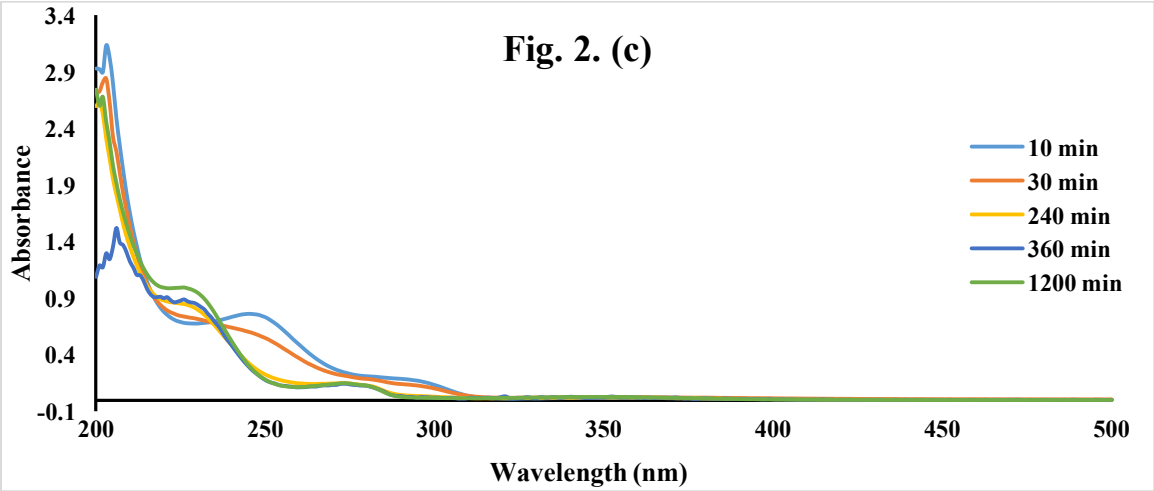

Fig. 2. UV-Vis spectra of 40 mg/L AMX at (a) pH 3.0, (b) pH 7.0 and (c) pH 11.0

From Fig. 2a – 2c, the test result suggested that at pH 3.0 and pH 7.0, the UV-Vis absorbance of AMX had no shift and was stable for at least 6 h. This time length was enough for the adsorption study in this experiment. Fig. 2c showed a shift of AMX absorbance along with time at pH 11.0 which suggest structural changes of AMX. This phenomenon was taken into account and avoided in the following experiment.

2.3.2. Stability test of H^+-PANI/SBA-15 and PANI/SBA-15 under different pH

H^+-PANI/SBA-15 and PANI/SBA-15 were made from mesoporous silica and polymer materials. There is a chance for them to release small particles into solution and interfere with AMX UV-Vis adsorption peak. Generally, small particles in UV-Vis will show responses and peaks around 200 ~ 250 nm and this range contains AMX's adsorption peak at 228 nm.

To avoid interference and errors, H^+-PANI/SBA-15 and PANI/SBA-15 were tested for particle release by adding them individually into deionized water and kept stirring during the test. The concentration of both H^+-PANI/SBA-15 and PANI/SBA-15 were 1 mg/mL and will keep consistent throughout the entire experiment. Hydrochloride acid (0.1 M) and sodium hydroxide solution (0.1 M) were used for balancing solution's pH. Samples (1 mL) were drawn intermittently (5 min, 10 min, 30 min, 60 min and 150 min) and centrifuged to get supernatant for UV-Vis and pH analysis. This sampling procedure was used throughout the entire experiment.

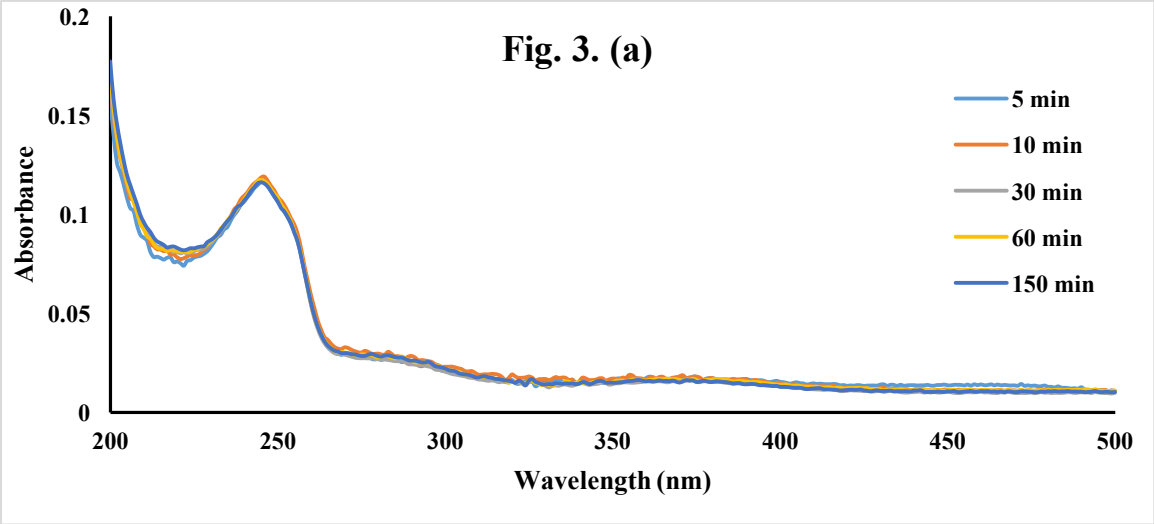
Fig. 3. (a)
Absorbance
0.2
0.15
0.1
0.05
0
200
250
300
350
400
450
500
Wavelength (nm)
5 min
10 min
30 min
60 min
150 min

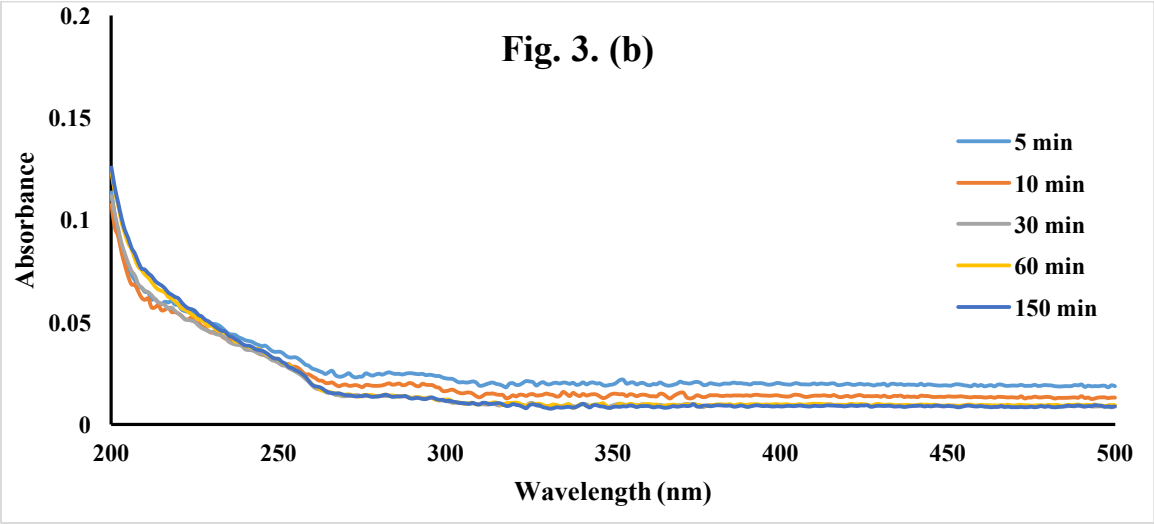
Fig. 3. (b)
Absorbance
0.2
0.15
0.1
0.05
0
200
250
300
350
400
450
500
Wavelength (nm)
5 min
10 min
30 min
60 min
150 min

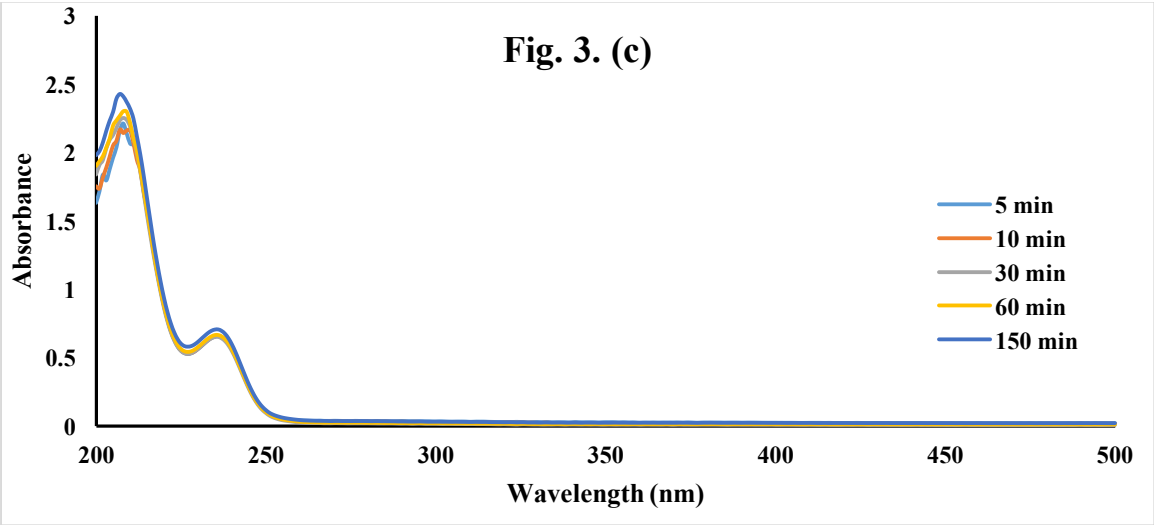
Fig. 3. (c)
Absorbance
3
2.5
2
1.5
1
0.5
0
200
250
300
350
400
450
500
Wavelength (nm)
5 min
10 min
30 min
60 min
150 min

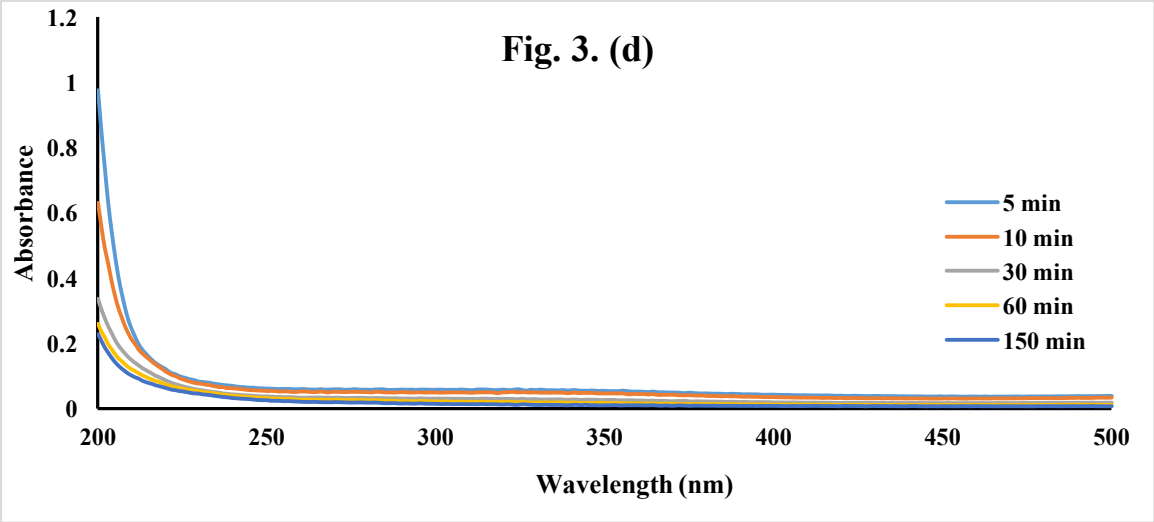

Fig. 3. UV-Vis spectra of (a) H^+-PANI/SBA-15 at pH 3.0, after 150 min, the pH became 2.9. (b) H^+-PANI/SBA-15 at pH 11.0, after 150 min, the pH became 6.0. (c) PANI/SBA-15 at pH 3.0, after 150 min, the pH became 3.8. (d) PANI/SBA-15 at pH 11.0, after 150 min, the pH became 8.3.

From the results above, it suggested that H^+-PANI/SBA-15 under pH 11.0 (Fig. 3b, pH after 150 min was pH 6.0, which can be considered as neutral) had very low absorbance profile on the UV-Vis spectra and had the least interfere with AMX's absorbance. While under other pH values, e.g. H^+-PANI/SBA-15 in pH 3.0 and PANI/SBA-15 in pH 3.0, the composite was not very stable and had some adsorption peaks within wavelength of 200 – 250 nm. The experiment result obtained afterward removed the effect from this test.

2.3.3. Standard curve for concentration of AMX versus absorbance

The absorbance of different concentrations (10, 20, 30, 40, 50 ,60, 70, 80, 90 and 100 mg/L) of AMX in deionized water was measured by UV-Vis spectroscopy within the range of 200 nm to 500 nm. The peak adsorption of AMX in UV-Vis occurs at 228 nm[15].

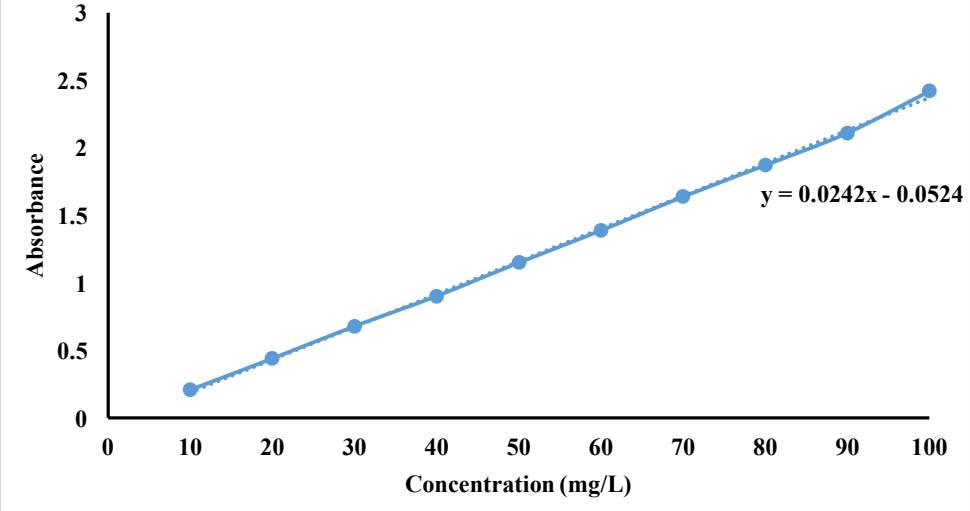

Fig. 4. Standard curve of AMX.

2.3.4. Batch adsorption study

The absorbent (H^+-PANI/SBA-15 and PANI/SBA-15) dosage used for all batch adsorption study was 1 mg/mL as well as solution's volume was fixed at 20 mL. For a typical procedure, different volumes of AMX stock solution were pipetted into beaker and then being diluted with deionized water to desired concentration with a fixed volume of 20 mL. Hydrochloride acid (0.1 M) and sodium hydroxide solution (0.1 M) were used for adjusting solution's pH to desired values. The absorbent (H^+-PANI/SBA-15 or PANI/SBA-15) of 20 mg was then quickly added to the solution and stirred for uniform adsorption. During the adsorption process, samples were pipetted at desired time point for UV-Vis analysis and then put back.

The concentration of AMX remained in the solution C_t (mg/L) at time t (min) was calculated by the AMX standard curve:

$$C_t = \frac{(A_t - A_c) + 0.0524}{0.0242} \quad (1)$$

where A_t is the absorbance of AMX at time t; A_c is the absorbance of nano composite (H^+-PANI/SBA-15 or PANI/SBA-15) in water without adding AMX.

The total mass of AMX being adsorbed onto adsorbent at time t, denoted as m_t (mg), was calculated by:

$$m_t = (C_0 - C_t)\, V \quad (2)$$

where C_0 (mg/L) is the initial concentration, V (L)is the volume of the solution.

2.3.4.1. AMX adsorption with H^+-PANI/SBA-15 and PANI/SBA-15 under different pH values

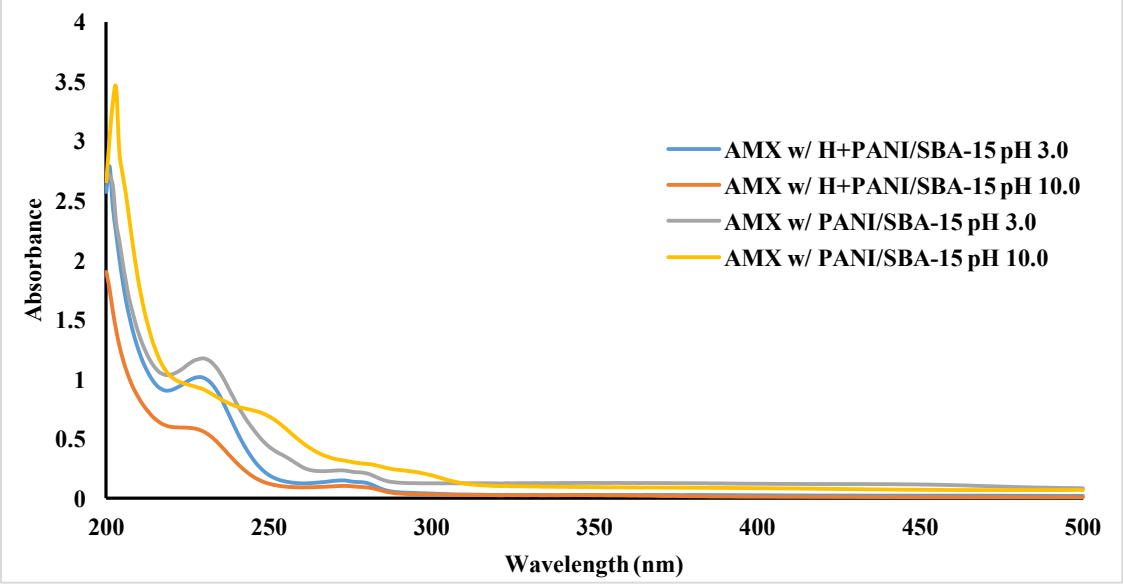

Fig. 5. UV-Vis spectra of AMX upon adsorption with H^+-PANI/SBA-15 or PANI/SBA-15 in deionized water after 6 h. The initial concentration of AMX solution was 40 mg/L.

Result comparison:

Table 1. pH_i is the initial pH of the solution; pH_f is the final pH of the solution; Removal % stands for the percentage of mass of AMX being removed from the initial mass of AMX in the solution.

	pH_i	**pH_f**	***C_t*** (mg/L)	***m_t*** (mg)	***Removal %***
AMX + H^+-PANI/SBA-15	3.0	3.0	39.2	0.02	2.5
AMX + H^+-PANI/SBA-15	10.0	7.0	21.8	0.36	45.0
AMX + PANI/SBA-15	3.0	4.0	43.5	-0.07	N/A
AMX + PANI/SBA-15	10.0	9.0	35.8	0.08	10

From the results above, it is obvious that AMX with H^+-PANI/SBA-15 at pH 10.0 was the most effective one. The other combinations did not show much or any signs of adsorption. What is worth notice is that the adsorption of AMX with H^+-PANI/SBA-15 started with initial pH at 10.0 and ended at pH 7.0. It may suggest that a neutral pH could help AMX being adsorbed better on H^+-PANI/SBA-15. One question that came up after this is that whether H^+-PANI/SBA-15 at pH 10.0 would be deprotonated to become PANI/SBA-15 (as a color change from dark green to blue was observed, indicating the possible deprotonation had taken place), which might also be the reason for the decrease in the value of pH. At this point, which material is actually adsorbing AMX is questionable. The following experiments were set up further to investigate the adsorption process.

2.3.4.2. Effect of pH and time on AMX adsorption with H^+-PANI/SBA-15

The adsorption time needed for AMX to reach balance was studied in this experiment. The concentration of AMX is 40 mg/L; Concentration of H^+-PANI/SBA-15 is 1 mg/mL; Solution volume is 20 mL.

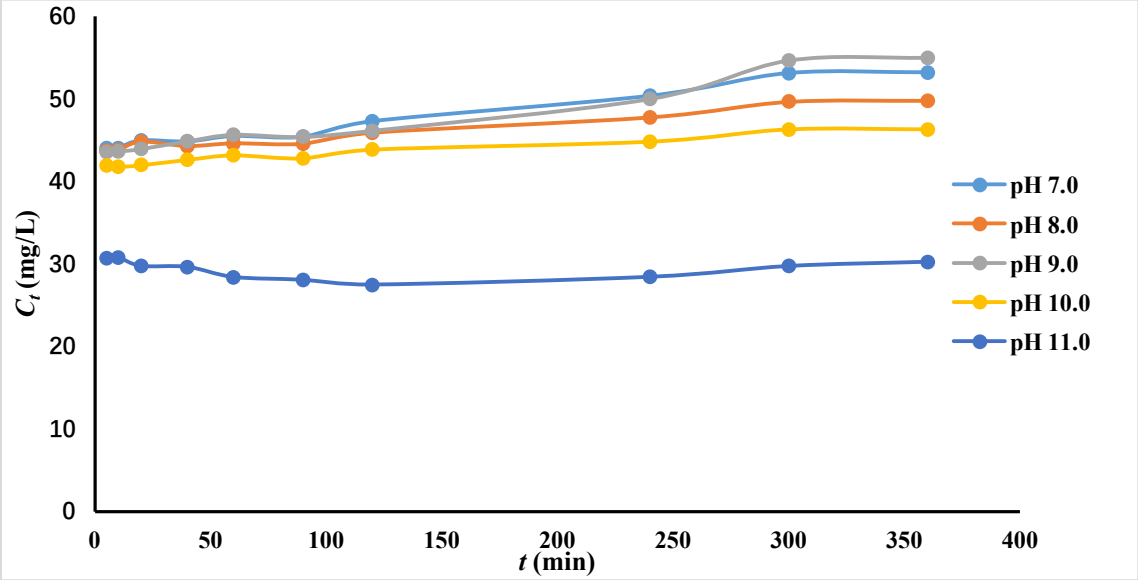

Fig. 6. UV-Vis spectra of AMX upon adsorption with H^+-PANI/SBA-15 varying with pH at different time points.

Result comparison:

Table 2. The details of AMX adsorption with H^+-PANI/SBA-15 variation with time at different pH values.

Initial pH	Final pH	C_t (mg/L)
7.0	3.4	47.3
8.0	3.7	45.9
9.0	3.6	46.1
10.0	4.7	43.8
11.0	7.5	27.5

By combining the results in Fig. 6, Table 2, there are some points can be discussed below:

(1) As shown from Fig. 6, the adsorptions of AMX with H^+-PANI/SBA-15 that took place between pH 7.0 – pH 10.0, all had their final AMX concentration higher than the initial concentration (40 mg/L). Based on the result from Fig. 2a and Fig. 2b, AMX didn't have adsorption peak shift within pH range of 3.0 to 7.0 and was very stable for at least 6 h. So the increase of concentration was not caused by AMX absorbance shift. It is possible that H^+-PANI/SBA-15 is responsible for the increase of AMX absorbance, because H^+-PANI/SBA-15 can release small particles into solution. Besides, Fig. 6 shows the increase of AMX concentration slowly went up with respect to time, which may indicate the buildup of small particles concentration. Moreover, stirring during adsorption process was set to keep the solution uniform and facilitate mass transfer, but it could also enhance the mechanical collision between H^+-PANI/SBA-15 particles and as a result the release of small particles.

(2) As we know, H^+-PANI/SBA-15 has the ability to increase solution's acidity (e.g. from pH 7.0 to pH 3.4) and this process takes place simultaneously as H^+-PANI/SBA-15 being mixed with AMX solution. The final pH of the solution should be as same as the pH of after H^+-PANI/SBA-15 has been completely mixed within the solution. So the adsorption process was actually taken place within the pH range of 3.4 to 7.5. In this way, the situation of unstable AMX UV-Vis absorbance at pH 11.0 (Fig. 2c) is avoided.

(3) Results from Fig. 6 indicated that the adsorption process had reached equilibrium in a very short time. The AMX concentration from first 5 min did not vary much compared with AMX concentration at 120 min. After 120 min, the effect of released

small particles from H^+-PANI/SBA-15 became stronger and interfered with AMX's absorbance at initial pH from 7.0 to 10.0. However, there is an exception of AMX adsorption at initial pH 11.0, where the AMX concentration kept nearly consistent through the entire experiment. The corresponding pH after adsorption was 7.5. Considering all these factors above, if the adsorption time take too long, small particles come off from H^+-PANI/SBA-15 will affect the AMX absorbance; on the other hand, enough time should be given to allow thorough mass transfer. As a result, the adsorption time for latter experiments was set to 2 h.

(4) By comparing results from Fig. 6 and Table 2, it was obvious to see the adsorption took place at initial pH 11.0 (with final pH 7.5) had the most AMX being adsorbed in H^+-PANI/SBA-15. Other samples (pH 7.0 – pH 10.0) also showed a tendency that the higher final pH value was the more AMX was adsorbed onto H^+-PANI/SBA-15. At this point, finding the optimum pH range that best promote AMX adsorption onto H^+-PANI/SBA-15 is important.

Two more adsorption data were collected separately at pH 12.0 and pH 13.0, results are shown below:

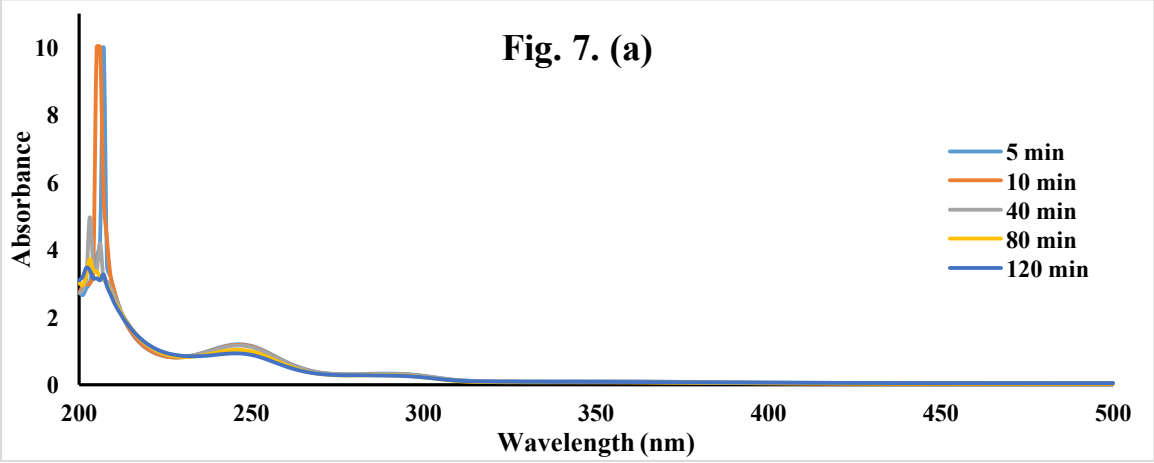

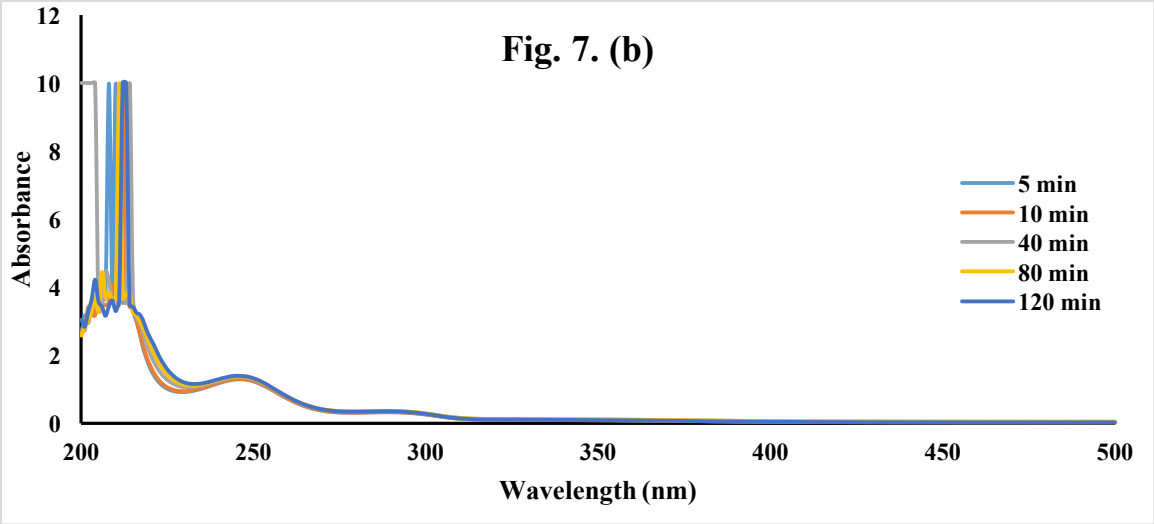

Fig. 7. UV-Vis spectra of 40 mg/L AMX with 1 mg/mL H^+-PANI/SBA-15 in 20 mL solution with (a) initial pH 12.0 and final pH 10.3. (b) initial pH 13.0 and final pH 12.6.

Both results (Fig. 7a and Fig. 7b) showed that there were many strong adsorption peaks in the range of 200 – 230 nm, which could attribute to small particles that came off from H^+-PANI/SBA-15. A difference between these two results was that the strong adsorption peaks in Fig. 7a were reduced dramatically over time while in Fig. 7b remained the same, which could be an indication that H^+-PANI/SBA-15 loses its integrity in basic environment. The results also indicated the adsorption peak of AMX had shifted from 228 nm to around 250 nm. This phenomenon was also observed in Fig. 2c. However, in Fig. 2c, the adsorption peak appeared only once at 250 nm for the first 10 min, then the peak started shifting back to 228 nm. Looking at the above factors, both AMX and H^+-PANI/SBA-15 were not stable in very basic conditions (e.g. above pH 11.0). Also, in reality, it is not common to find very basic conditions either in nature environment or living organisms. Therefore, very basic conditions will not be further tested in this experiment.

2.3.4.3. Effect of initial concentration and time on adsorption capacity

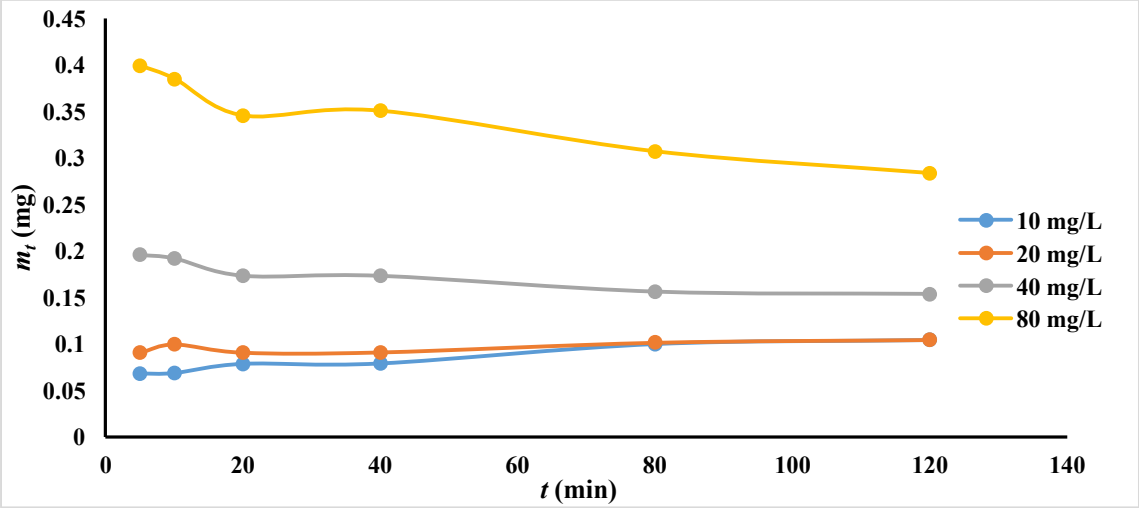

Fig. 8. Amount of AMX adsorbed on H^+-PANI/SBA-15 at pH 11.0 from solutions with different initial concentration of AMX. The final pH was in the range of 8.0 – 8.2.

Fig. 8 shows that the increase of initial AMX concentration will also increase the amount of AMX adsorbed on H^+-PANI/SBA-15. However, the percentage ($\frac{m_e}{m_i}$, m_e is the mass of adsorbed AMX at equilibrium, m_i is the mass of AMX in initial solution) of adsorbed AMX had dropped greatly (from 50% to 17.5%), which indicated the adsorption capacity of H^+-PANI/SBA-15 was getting saturated. As the AMX initial concentration went higher, the amount of adsorbed AMX tend to drop to some extent. This phenomenon can be explained by that as more AMX adsorbed onto H^+-PANI/SBA-15, the adsorption sites will get saturated and some AMX molecules were loosely bind or trapped within the pores of H^+-PANI/SBA-15. The mechanical collision of H^+-PANI/SBA-15 molecules caused by continuous stirring will releases some adsorbed AMX molecules back into the solution, plus the AMX molecules which were initially trapped within the pores will re-enter solution over time, the amount of adsorbed AMX will decrease.

2.3.4.4. Adsorption of AMX with PANI/SBA-15

In previous experiments, it was observed that H^+-PANI/SBA-15 was effective in adsorbing AMX under certain pH values (e.g. with initial pH around 11.0 and final pH around 7.0 – 8.0). As analyzed before, H^+-PANI/SBA-15 will undergo transformation to become PANI/SBA-15 in basic solution. This was proved by the fact that the color of the solution will change from dark green to dark blue, which are the color for H^+-PANI/SBA-15 and PANI/SBA-15 respectively. To this point, a question was raised about which material (H^+-PANI/SBA-15 or PANI/SBA-15) was actually adsorbing AMX.

To answer this question, a comparative study was set to test the adsorptive ability of PANI/SBA-15 on AMX. In this experiment, the amount of PANI/SBA-15 was set at 1 mg/mL in the initial AMX concentration of 40 mg/L at room temperature. Because PANI/SBA-15 won't affect pH value above 7.0, two pH values, pH 7.0 and pH 8.0, were chosen for this experiment in order to keep consistent with the final pH values from previous experiments.

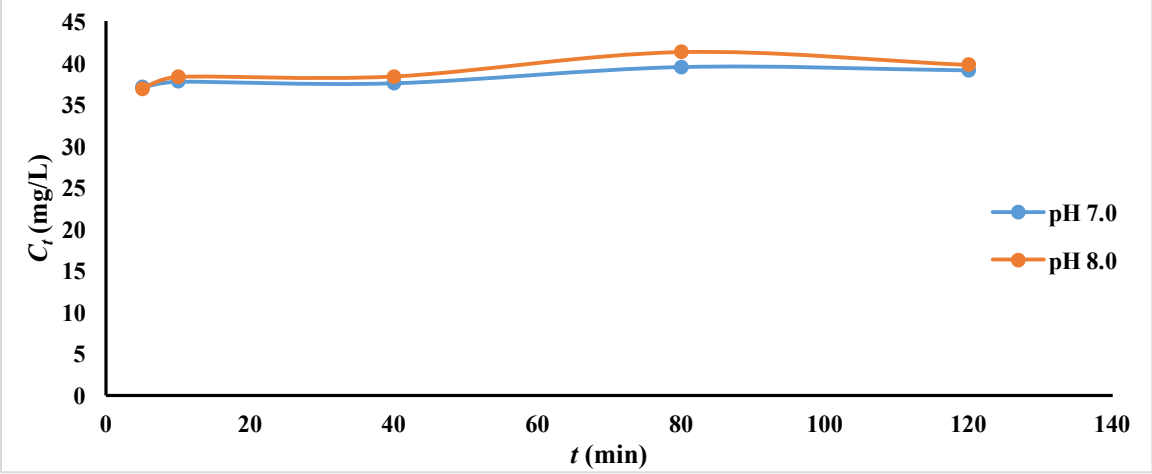

Fig. 9. Concentration change of 40 mg/L AMX with 1 mg/mL PANI/SBA-15 in 20 mL solution. When the initial pH is 7.0, the final pH reaches 7.3 and when the initial pH 8.0, the final pH turns to 7.5.

The result from Fig. 9 shows that there is not much difference between the initial AMX concentration and final AMX concentration in the solution. In another word, PANI/SBA-15 did not adsorb AMX at pH 7.0 and pH 8.0. This proves that in previous experiments, H^+-PANI/SBA-15 was the material adsorbing AMX.

2.4. Adsorption Kinetic Study

In order to get a more comprehensive understanding of adsorption of AMX in H^+-PANI/SBA-15, kinetic behavior was studied by setting the amount of H^+-PANI/SBA-15 at 1 mg/mL and AMX initial concentration at 40 mg/L at room temperature.

The amount of AMX adsorbed at equilibrium q_e (μg/mg) on the adsorbents was calculated with the following equation:

$$q_e = \frac{m_e}{W} \tag{3}$$

where m_e has the same meaning as previously mentioned, W is the mass of adsorbent used (mg).

The amount of AMX adsorbed in H^+-PANI/SBA-15 at time t, q_t (μg/mg) was calculated by:

$$q_t = \frac{m_t}{W} \tag{4}$$

where m_t has the same meaning as in equation (2).

Pseudo-second order and intraparticle diffusion models were tested on the adsorption data obtained for AMX adsorption with H^+-PANI/SBA-15. The validity of the models was checked by linear equation analysis of t/q_t *vs* t, and q_t *vs* $t^{0.5}$ and their corresponding correlation coefficients, R^2.

2.4.1. Pseudo-second order

The pseudo-second order kinetic rate equation is expressed as[16]:

$$\frac{dq_t}{dt} = k_2(q_e - q_t)^2 \tag{5}$$

where k_2 is the rate constant of pseudo-second order adsorption (mg/μg min). After

integrating and rearranging equation (5) using the boundary conditions $t = 0$ to $t = t$ and $q_t = 0$ to $q_t = q_t$, the following equation can be obtained:

$$\frac{t}{q_t} = \frac{1}{k_2 q_e^2} + \frac{t}{q_e} \quad (6)$$

If pseudo-second order kinetics is applicable, the plot of t/q_t *vs* t should give a linear relationship, and q_e (calculated) and k_2 can be determined from the slope and intercept of the plot, respectively).

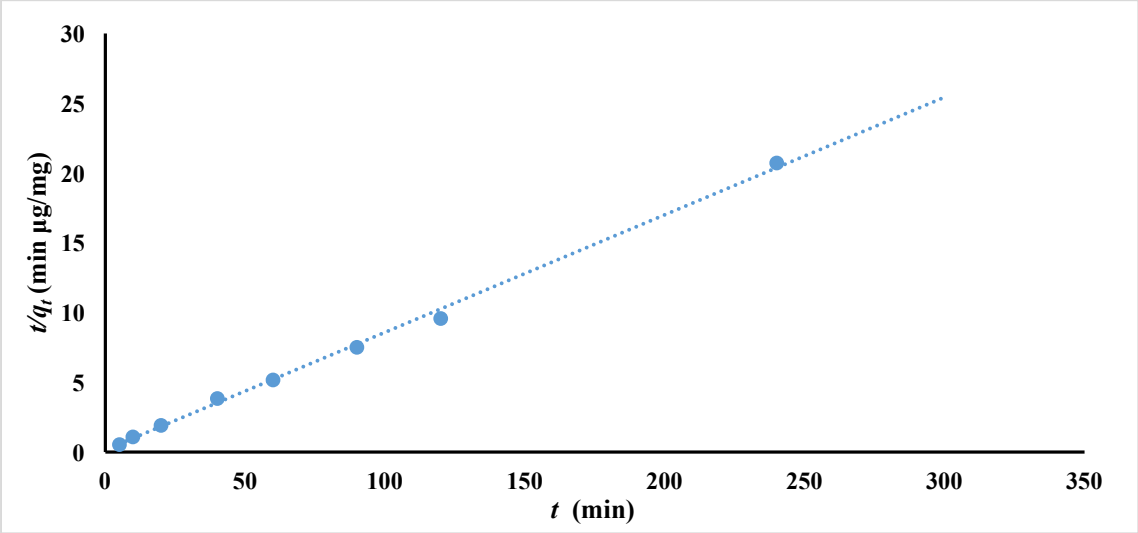

Fig. 10. Pseudo-second order model-based plots of the adsorption of AMX in H^+-PANI/SBA-15. Kinetic data: q_e (calculated) = 11.86 (µg/mg), q_e (experiment) = 11.59 (µg/mg), k_2 = 0.053 (mg/µg min), R^2 = 0.998.

2.4.2. Intraparticle diffusion model

Intraparticle diffusion model was designed by Weber and Morris and the equation is as follow:

$$q_t = k_i t^{0.5} + C \quad (7)$$

where k_i is the intraparticle diffusion rate constant in µg/mg $min^{0.5}$ and C is a y-intercept

(μg/mg), which is proportional to the boundary layer thickness. If the intraparticle diffusion is the rate-controlling factor, then the plot of q_t *vs* $t^{0.5}$ should be linear. Moreover, if the plot passes through the origin, then the intraparticle diffusion can be said to be the only rate-limiting factor.

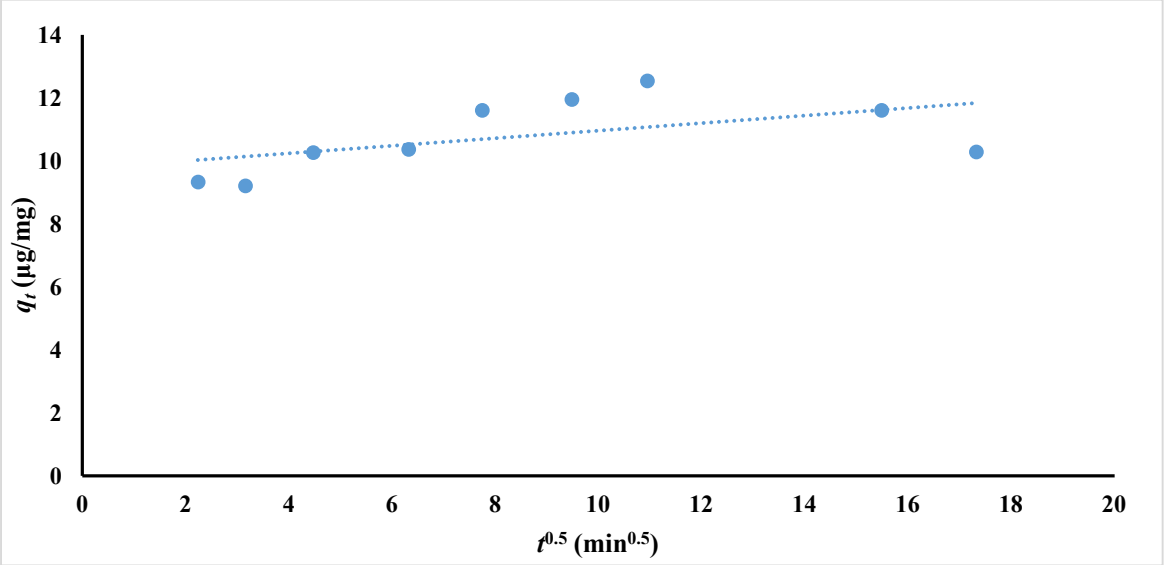

Fig. 11. Intraparticle diffusion model-based plots of the adsorption of AMX in H^+-PANI/SBA-15. Kinetic data: $k_i = 0.12$, $R^2 = 0.285$.

By comparing the results of these two models above, we could probe the mechanism of adsorption in this experiment. The data from Fig. 10, pseudo-second order model, showed the R^2 value was close to one and the calculated adsorption capacity was similar with experimental data. On the other hand, the intraparticle model had a very low R^2 value and the plot was not linear as well. Therefore, pseudo-second order model becomes the best model describing AMX and H^+-PANI/SBA-15 adsorption process. This result also suggested that chemisorption played an important role in the rate-controlling step.

So far, after taking each result into consideration, one possible explanation of the

adsorption process was through the combination of hydrogen bond and electrostatic attraction. Start with AMX chemical structure, the coexistence of carboxyl (–COOH, pKa_1 = 2.68), amine (–NH_2, pKa_2 = 7.49) and phenolic (–OH, pKa_3 = 9.63) functional groups endow AMX molecules different ionization forms under different pH values. At pH < pKa_1 the AMX groups will be protonated as –COOH/–NH_3^+/–OH (AMX^+); at pH values between pKa_1 and pKa_2 the carboxylic group will be deprotonated as –COO^-/–NH_3^+/–OH ($AMX^\pm$); at pH values between pKa_2 and pKa_3 both carboxylic and amine groups will be deprotonated to –COO^-/–NH_2/–OH (AMX^-); at pH > pKa_3 the phenolic hydroxyl will also be deprotonated –COO^-/–NH_2/–O^- (AMX^{2-}). In this experiment, when at the most effective pH value 11.0, AMX^{2-} was the dominant specie. When H^+-PANI/SBA-15 was added into the solution, electrostatic attraction was generated between those two molecules and AMX^{2-} was then adsorbed on H^+-PANI/SBA-15. Moreover, since there were lots of oxygen and nitrogen atoms existing in both AMX and H^+-PANI/SBA-15, hydrogen bond was very likely to form.

2.5. Conclusion

H^+-PANI/SBA-15 and PANI/SBA-15 materials were successfully synthesized, and their efficacy in adsorbing AMX under different pH values were evaluated. It was found that the adsorption of AMX in H^+-PANI/SBA-15 was pH sensitive and would achieve the best adsorption with pH, which started at 11.0 (basic) and stabilized around 7.0 (neutral). The initial AMX concentration could affect total amount of AMX that adsorbed in H^+-PANI/SBA-15. Within the range of tested concentration, the higher initial concentration was, the more AMX could be adsorbed. On the contrary, PANI/SBA-15 did not show signs of adsorption of AMX in the experiment. Two adsorption kinetic models were fitted to experiment data, the pseudo-second order model and intraparticle model. The parameters from these two models suggested that the pseudo-second order model fitted well with experimental data, which indicated chemisorption was involved during the adsorption process. One possible explanation of the adsorption process has been proposed, but due to the complexity of adsorption itself, further studies on the adsorbing mechanism is encouraged. We hope our results could support further researches on the adsorption of emerging pollutants and other chemicals by porous inorganic/polymer hybrid nanomaterials.

References

1. Buzea, C., Pacheco, I. I., & Robbie, K. (2007). Nanomaterials and Nanoparticles: Sources and Toxicity. Biointerphases, 2(4), MR17-MR71.

2. Eric, D. K. (1986). Engines of Creation. The Coming Era of Nanotechnology. Anchor Book.

3. Drexler, K. Eric (1992). *Nanosystems: Molecular Machinery, Manufacturing, and Computation*. New York: John Wiley & Sons. ISBN 0-471-57547-X.

4. Geissen, V., Mol, H., Klumpp, E., Umlauf, G., Nadal, M., van der Ploeg, M., ... & Ritsema, C. J. (2015). Emerging Pollutants in the Environment: A Challenge for Water Resource Management. International Soil and Water Conservation Research, 3(1), 57-65.

5. Escher, B. I., Baumgartner, R., Koller, M., Treyer, K., Lienert, J., & McArdell, C. S. (2011). Environmental Toxicology and Risk Assessment of Pharmaceuticals from Hospital Wastewater. Water Research, 45(1), 75-92.

6. González-Pleiter, M., Gonzalo, S., Rodea-Palomares, I., Leganés, F., Rosal, R., Boltes, K., ... & Fernández-Piñas, F. (2013). Toxicity of five antibiotics and their mixtures towards photosynthetic aquatic organisms: implications for environmental risk assessment. Water Research, 47(6), 2050-2064.

7. Pouretedal, H. R., & Sadegh, N. (2014). Effective Removal of Amoxicillin, Cephalexin, Tetracycline and Penicillin G from Aqueous Solutions Using Activated Carbon Nanoparticles Prepared from Vine Wood. Journal of Water Process Engineering, 1, 64-73.

8. Kanakaraju, D., Kockler, J., Motti, C. A., Glass, B. D., & Oelgemöller, M. (2015). Titanium Dioxide/Zeolite Integrated Photocatalytic Adsorbents for the Degradation of Amoxicillin. Applied Catalysis B: Environmental, 166, 45-55.

9. Merlin, C., Bonot, S., Courtois, S., & Block, J. C. (2011). Persistence and Dissemination of the Multiple-antibiotic-resistance Plasmid pB10 in the Microbial Communities of Wastewater Sludge Microcosms. Water Research, 45(9), 2897-2905.

10. Okamoto, Yoshikuko and Brenner, Walter (1964) "Polymers", Ch. 7 pp. 125–158 in Organic Semiconductors, Reinhold.

11. Mahanta, D., Madras, G., Radhakrishnan, S., & Patil, S. (2009). Adsorption and Desorption Kinetics of Anionic Dyes on Doped Polyaniline. The Journal of Physical Chemistry B, 113(8), 2293-2299.

12. Malinauskas, A. (2001). Chemical Deposition of Conducting Polymers. Polymer, 42(9), 3957-3972.

13. Zhang, T., Huang, X., & Asefa, T. (2015). Nanostructured Polymers with High Surface Area Using Inorganic Templates for the Efficient Extraction of Anionic Dyes from Solutions. Chemical Communications, 51(89), 16135-16138.

14. Gholivand, M. B., Abolghasemi, M. M., & Fattahpour, P. (2012). Highly Porous Silica-polyaniline Nanocomposite as a Novel Solid-phase Microextraction Fiber Coating. Journal of Separation Science, 35(1), 101-106.

15. Pezoti, O., Cazetta, A. L., Bedin, K. C., Souza, L. S., Martins, A. C., Silva, T. L., Almeida, V. C. (2016). NaOH-activated Carbon of High Surface Area Produced from Guava Seeds as a High-efficiency Adsorbent for Amoxicillin Removal: Kinetic, Isotherm and Thermodynamic Studies. Chemical Engineering Journal, 288, 778-788.

16. Namasivayam, C., & Kavitha, D. (2002). Removal of Congo Red From Water by Adsorption Onto Activated Carbon Prepared from Coir Pith, An Agricultural Solid Waste. Dyes and Pigments, 54 (1), 47-58.